

Spatially Resolved Quantum Nano-Optics of Single Photons Using an Electron Microscope

L. H. G. Tizei and M. Kociak*

Laboratoire de Physique des Solides, Université Paris-Sud, CNRS-UMR 8502, Orsay 91405, France
(Received 3 January 2013; revised manuscript received 15 February 2013; published 9 April 2013)

We report on the experimental demonstration of single-photon state generation and characterization in an electron microscope. In this aim we have used low intensity relativistic (energy between 60 and 100 keV) electrons beams focused in a ca. 1 nm probe to excite diamond nanoparticles. This triggered individual neutral nitrogen-vacancy centers to emit photons which could be gathered and sent to a Hanbury Brown-Twiss intensity interferometer. The detection of a dip in the correlation function at small time delays clearly demonstrates antibunching and thus the creation of nonclassical light states. Specifically, we have also demonstrated single-photon states detection. We unveil the mechanism behind quantum states generation in an electron microscope, and show that it clearly makes cathodoluminescence the nanometer scale analog of photoluminescence. By using an extremely small electron probe size and the ability to monitor its position with subnanometer resolution, we also show the possibility of measuring the quantum character of the emitted beam with deep subwavelength resolution.

DOI: [10.1103/PhysRevLett.110.153604](https://doi.org/10.1103/PhysRevLett.110.153604)

PACS numbers: 42.50.Dv, 07.78.+s, 42.50.Ar, 78.60.Hk

The study of single-photon sources has attracted great attention [1–10]. The interest in these emitters stems from the mandatory requirement to create optical states which are fundamentally different from classical ones for fundamental [8] or technologically important applications, such as quantum computing and quantum cryptography [9,10]. Reliable single-photon sources (SPS) have been demonstrated based, among others, on nitrogen-vacancy (NV) centers in diamond, which have been extensively studied using photoluminescence (PL) [6] and in a lesser extent using electroluminescence (EL) [7] techniques.

After excitation of an SPS, the probability of detecting two simultaneous photon emissions is zero, independently of the exciting probe statistics. This amazing quantum effect is called photon antibunching. Its observation unambiguously confirms the detection of quantum states of light. Single-photon states can be evidenced by measuring the second order correlation function, $g^{(2)}(\tau)$. This function,

$$g^{(2)}(\tau) = \frac{\langle I(t)I(t+\tau) \rangle}{\langle I(t) \rangle \langle I(t+\tau) \rangle}, \quad (1)$$

provides information about intensity $[I(t)]$ correlations of a given light field at different time delays, τ . It can be measured using a Hanbury Brown-Twiss [11] (HBT) intensity interferometer (see below and Fig. 1). For classical light, $g^{(2)}(\tau) \geq 1$ for any τ . However, for a single-photon beam, $g^{(2)}(0) = 0$ [2,6]. That is, given that a detection event has taken place, the probability of a second detection (for times shorter than the lifetime of the emitter) is lower than that for classical light. More generally, $g^{(2)}(0)$ scales as $(1 - 1/n)$, where n is the number of photons in the state.

The requirement for the emission of one photon at a time implies that the emitting object will be ideally a two levels system in which saturation effects ensures that the system

cannot be reexcited unless a photon is previously emitted. Thus, generally an SPS will have a limited size: an atom (e.g., Cs atoms in an optical cavity [12]), a point defect (e.g., a NV center in bulk diamond [6]), or a quantum dot (e.g., GaN in a AlN matrix [13] or CdSe nanocrystals [14]), etc. Incidentally, conventional optical techniques, being diffraction limited [15], will probe single objects only in highly dispersed samples. Subwavelength photon-based microscopy may suffer from other limitations: scanning near field optical microscopy signals decrease rapidly with spatial resolution [16] and stimulated emission depletion microscopy cannot selectively excite multiple quantum emitters inside small objects [17,18]. However, advances in the understanding of the physics of light at nanometric scales are clearly desirable. Using fast electrons to trigger photon emission (cathodoluminescence [19], CL) is an ideal candidate for such experiments, due to the nowadays proved nanometric spatial resolution [20]. Indeed, CL has been used to study either quantum dots [21–23] or point defects such as NV centers [24,25]. However, only very few studies could address individual objects [20,25], and, more importantly, none has reported the measurement of antibunching, which is yet the definite signature of a SPS. Hence, techniques assessing quantum optics at the scales relevant to many objects and at which their interactions take place are necessary.

In this Letter, to circumvent the described limitations, we have used a radically different approach to the pure optical means. We have demonstrated the use of fast electrons (relativistic particles with energy set between 60 and 100 keV) focused in a ≈ 1 nm-wide beam formed in a scanning transmission electron microscope (STEM) to excite neutral (NV⁰) centers in diamond nanoparticles and prove that they can trigger single-photon (SP) emission. The experiments described here were performed at

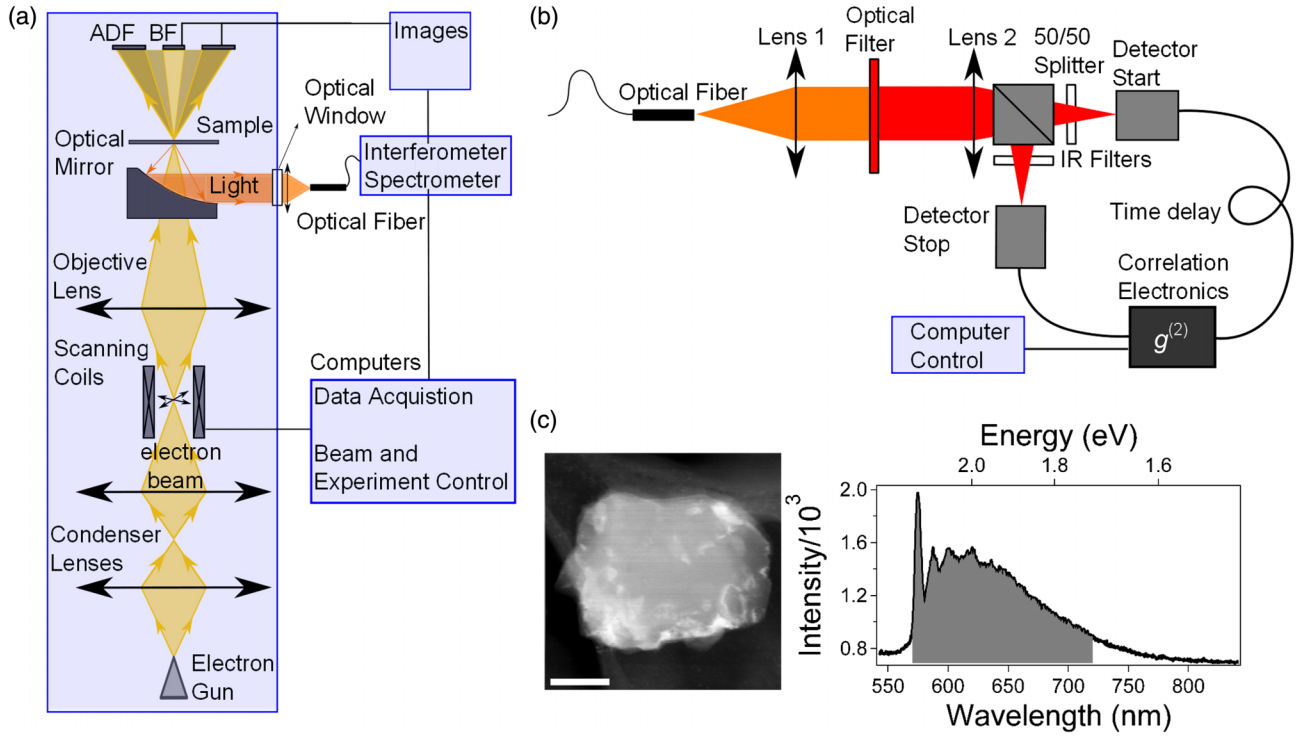


FIG. 1 (color online). (a) A light collection system was installed in a STEM microscope: a parabolic mirror collects the light emitted during electron irradiation, which is focused by a lens onto an optical fiber. This fiber is coupled to a spectrometer or to a HBT interferometer. (b) HBT interferometer. (c) ADF image of a diamond particle and a spectrum of light emitted from a particle containing NV⁰ centers, detected between 570 and 720 nm (gray area). The spectrum shows the NV⁰ zero-photon line at 575 nm and the associated phonon lines at longer wavelengths. The scale bar in (c) is 100 nm.

80 keV. The deexcitation mechanism is evidenced to be equivalent to that of photoluminescence through the centers lifetime. It indicates that cathodoluminescence at the nanometer scale can be seen as a broadband analog of photoluminescence rather than electroluminescence. We also showed that the excitation position can be controlled to allow the deep subwavelength characterization of the quantum character of the emitted states.

The experiments have been performed in a VG HB 501 STEM microscope with in-house made scanning electronics. This microscope is equipped with a liquid nitrogen cooled sample stage. Light (CL) was collected with a carefully optimized high efficiency collection system [20], which was crucial to the success of the experiments. Light was coupled to a HBT interferometer [11] or a spectrometer [Figs. 1(a) and 1(b)] using an optical multi-mode fiber (100 μm diameter core). Single photons have been detected by two Picoquants τ -SPADs (single photon avalanche diodes). Time-delay histograms (which are proportional to the second order correlation function) have been acquired using the Time Harp correlation electronics, from Picoquant. The typical room background noise varied between 100 and 500 count/s. Wavelength filtered images have been acquired by measuring a SPAD count signal. The typical acquisition time for each correlation curve was 300 s. Time delay histograms have been normalized to one for $\tau \gg 0$. This is justified by the shape of the curves, which do not show a bunching effect. Opposite to conventional

PL, standard background subtraction has not been performed because it cannot be estimated from the collected data. Light intensity and statistics are not constant within a particle, rendering unjustifiable the usual [6,26] subtraction of a Poissonian background without further information. At each position of a scan of the electron beam, two structural signals (annular dark field, ADF, roughly proportional to the projected mass, and bright field, BF), the light emission spectra [Fig. 1(c)] or the $g^{(2)}(\tau)$ can be acquired in parallel. This allows the localization, with nanometer accuracy and without any ambiguity, of the light emission property within the object of interest (For example, using this setup without the HBT interferometer we have recently investigated different color centers in diamond nanoparticles [25]). In other words, it gives access to the advantages of well-established electron microscopy techniques and a quantum optic setup in a single experiment. To extract the antibunching dip depth, histograms have been fitted to the following model [26]:

$$g^{(2)}(\tau) = \begin{cases} 1 - ge^{-(\tau-\tau_0)/\Gamma} & \text{if } \tau \geq 0 \\ 1 - ge^{(\tau-\tau_0)/\Gamma} & \text{if } \tau < 0, \end{cases} \quad (2)$$

where $(1 - g)$ is the depth of the antibunching dip, Γ is the deexcitation lifetime of the center and τ_0 is the position of the minimum value of the $g^{(2)}(\tau)$ function.

Two kinds of nanoparticles have been used: (i) a sample of large diamond particles (larger than 500 nm) crushed

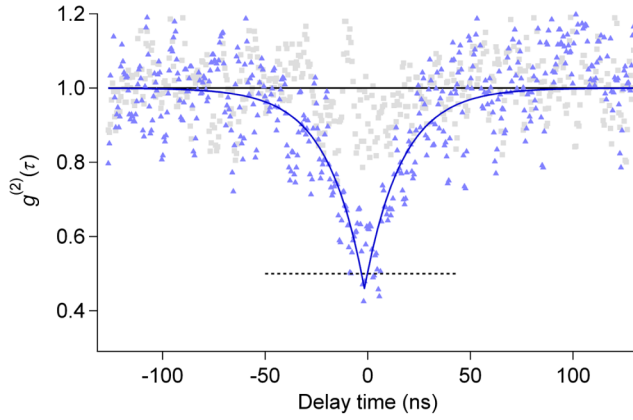


FIG. 2 (color online). $g^{(2)}(\tau)$ curves measured in two different nanoparticles excited by fast electrons. The black curve was measured in a particle emitting 100×10^3 count/s and does not show light antibunching. The blue curve was measured in a particle emitting $30\text{--}40 \times 10^3$ count/s and clearly shows light antibunching. This is a clear signature of the quantum nature of the light beam. As $g^{(2)}(0) = (0.46 \pm 0.05)$ this also demonstrates the detection of a single-photon emitter in the diamond lattice. The acquisition time for the blue and black curves was 250 and 300 s, respectively.

using a mortar (Aldrich), and (ii) a sample with diamond nanoparticles in the 100 to 200 nm range (Microdiamant). Both samples have been diluted in deionized water and dispersed on holey-carbon copper grids. Among those nanoparticles, for the presented experiments, SP candidates

have been chosen based on emission intensity in the wavelength range of interest. After each measurement an ADF image was acquired to check that the nanoparticle had not drifted.

We could observe two different statistical properties for the investigated particles. $g^{(2)}(\tau)$ measured from bright diamond nanoparticles (100×10^3 count/s per detector or more) are flat [$g^{(2)}(\tau) = 1$] within our experimental time resolution (around 350 ps). Such behavior indicates a classical source; see the black curve of Fig. 2. On the other hand, measurements on nanoparticles with weaker light emission (ca. 30×10^3 count/s) show antibunching (blue curve in Fig. 2). This undoubtedly demonstrates the detection of nonclassical light generated by fast electrons, which has not been reported so far to the best of our knowledge. The observation of classical curves in exactly the same experimental conditions, but for other nanoparticles, guarantees that the observed antibunching is not an effect of the electron beam statistics. The electron beam was maintained scanning a small fixed area (30 by 34 nm wide) on the nanoparticle [small blue rectangle on Fig. 3(a)]. The difference between the two statistical behaviors can be explained as due to different concentrations of NV^0 , or other centers, following the behavior in PL and EL experiments in which antibunching is seen only when a few NV^0 centers are excited (and in the absence of other centers).

We measured $g^{(2)}(0) = (0.46 \pm 0.05)$ for the blue curve. As a general statement, $g^{(2)}(0) < 0.5$ is the demonstration

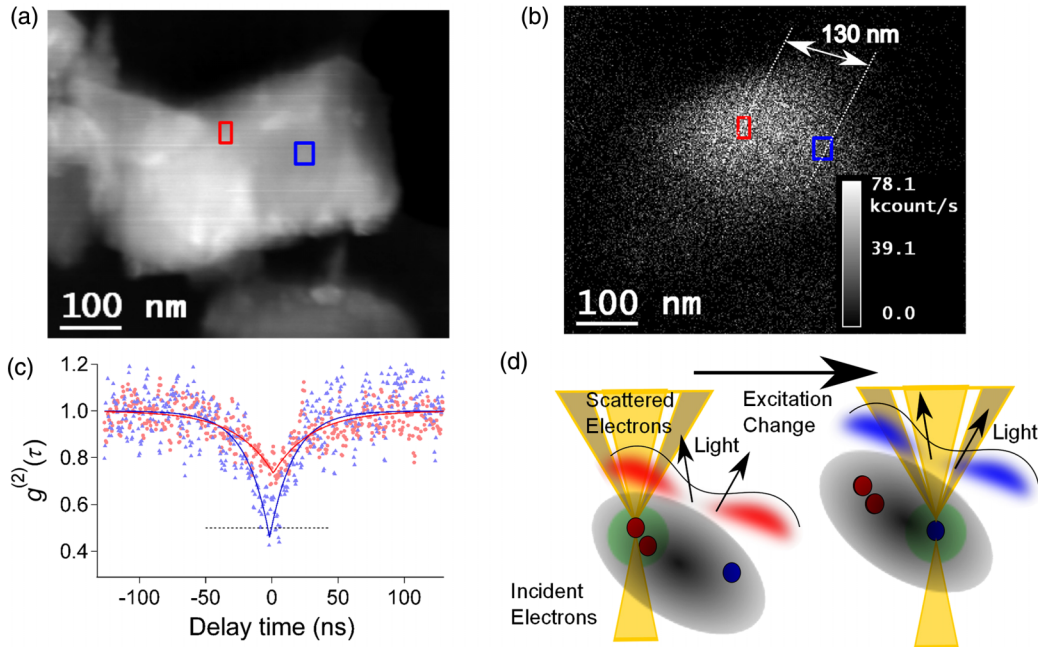


FIG. 3 (color online). (a) ADF and (b) integrated light intensity images of a diamond nanoparticle acquired in parallel (exposure time $64 \mu\text{s}$ per pixel). Light emission is not homogeneous through the particle. (c) $g^{(2)}(\tau)$ acquired with the electron beam scanning different regions (symbols represent data and lines fits), separated by 130 nm and marked by rectangles of the corresponding colors. The measured $g^{(2)}(0)$ values are (0.46 ± 0.05) and (0.73 ± 0.02) . The acquisition time for the blue and red curves was 250 s. (d) An electron beam excites a volume, defined by the electron probe and diffusion of carriers (light green circle). By shifting the probe one can excite light emission from another region, with possibly corresponding different $g^{(2)}(\tau)$ value.

that a beam of single photons has been detected. In the present case, this measurement unambiguously shows that we have detected single-photon states emitted from a diamond nanoparticle excited by a nanometer-wide fast electron beam. The nonzero value can be explained by the presence of a background signal [26]. In our experiment, the main origin of the background is the excitation of other centers due to charge carrier diffusion [25]. The deduced lifetime, $\Gamma = (18 \pm 4)$ ns is compatible with values for NV^0 centers in nanodiamond obtained by PL measurements and is a fundamental difference between the presented experiments and EL [7] in NV^0 centers.

The remarkable similarities between the present experiments and PL are explained by the fact that fast electrons interact with the sample during a few femtoseconds, creating neutral electron-hole pairs. Because of the electrons high speed and the thin samples used (contrary to conventional CL schemes in scanning electron microscope, SEM, on thick samples), the inelastic interaction is very small, leading to the creation of typically zero or one electron-hole pair above the diamond energy band gap per incident electron. The typical current in our experiments is of the order of 100 pA, or 1.6 electron every nanosecond. Thus, the time between two electrons is an order of magnitude shorter than the NV^0 typical lifetimes. In this sense, the excitation of the NV^0 center can be seen as continuous. The electron-hole pair rapidly (few picoseconds [27]), loses energy to reach the bottom (top) of the conduction (valence) band. It may then diffuse up to an emission center, where the electron-hole pair can excite the localized excited state of the NV^0 center much like a photon would directly excite the phonon-broadened energy levels. This creates a region around the center from which it can be excited, giving rise to maxima in light emission, as observed in previous experiments [25].

Of course, the measurement of $g^{(2)}(0) < 1$ on an individual particle can also be achieved by optical techniques provided it is well separated from its neighbors. However, optical techniques do not give access to information about variations of the $g^{(2)}(\tau)$ within the same nanoparticle, or more generally at deep subwavelength spatial resolution, nor do they give parallel access to the nanometer resolved image. Here, the excitation by fast electrons focused into a small probe onto a thin specimen provides the breakthrough needed to measure these variations.

This unique capability to monitor the excitation position with subwavelength resolution on a nanostructure imaged in parallel is the key difference between the excitation of color centers using a fast electron beam and a laser [explained in Fig. 3(d)]. The same advantage has been recently demonstrated in electron optical absorption experiments (electron energy-loss spectroscopy) [28,29] or classical luminescence experiments in an electron microscope [20].

To evidence this advantage we have measured $g^{(2)}(\tau)$ at a second area (20 by 34 nm) on the very same diamond

nanoparticle, separated by 130 nm from the first area [both marked on Figs. 3(a) and 3(b)]. The separation between these positions is about $\lambda/5$ (λ the wavelength of light). The values of $g^{(2)}(\tau = 0)$ are (0.46 ± 0.05) and (0.73 ± 0.02) , respectively [Fig. 3(c)]. The second value might be associated with a light emitted by two NV^0 centers, or one NV^0 center and some other potentially non-SP emitter centers emitting at the same wavelength, as the antibunching dip should be shallower in these cases. This shows the remarkable ability to measure the temporal statistics properties of nonclassical light beams excited from two distinct positions separated by subwavelength distances within the same nano-object. Moreover, this result proves that individual point defects can be detected with high-spatial resolution using cathodoluminescence, as previously conjectured by us [25]. The described excitation scheme, together with the here proven SP detection mimicking closely PL experiments, and the demonstrated spatial resolution sets CL in a STEM as the nanometre scale counterpart of PL.

The results presented here open the way to new research paths. From one perspective, we have demonstrated the ability to identify and count quantum emitters in close proximity and to measure their individual responses. These emitters could be any SPS, such as quantum dots [21,22] or NV^- (charged NV centers) centers [30] which have been observed using cathodoluminescence. This will allow a much better understanding of the physics of interaction between two or more emitters, should they be point defects, atoms, or densely packed quantum dots [13,14]. For example, one may probe how the $g^{(2)}(\tau)$ function varies spatially as the excitation probe is scanned between two centers. This would render feasible new, otherwise impossible, quantum nano-optics experiments. In particular, the here proven spatial resolution is limited by the diffusion distance, which is typically here less than 100 nm [25], but resolutions down to 5 nm are expected for other nanostructured systems [20]. Such a spatial resolution may allow the unique capability to image, to characterize, and to address individual quantum bits in compact systems. In addition to pure imaging, electron microscopes now allow the study of chemical, electronic, magneto-, and electrostatic properties of materials at the atomic scale, that could be used in parallel to $g^{(2)}(\tau)$ measurements. Naturally, such a possibility would aid the characterization of a future scalable quantum computing system.

Furthermore, our experiments reveal the emission of single-photon fields excited by fast electrons. Therefore, our work represents a new approach to the generation of single-photon states and could be applied to the study of electron-photon entanglement, as proposed recently [31]. Finally, the use of a pulsed electron source [23,32–34] could lead to the creation of nanometer sized triggered SPS. We believe that this experimental approach may have a significant impact in SPS studies, just as electron energy-loss studies have greatly aided the comprehension of plasmon physics in metallic nano-objects.

Finally, fast electrons couple effectively to plasmons in nanometer wide dissipative metallic particles [28,29]. Therefore, the study of the temporal statistics of light beams using fast electrons may allow new experiments in quantum plasmonics at the nanometer scale, in analogy to experiments performed using standard optical techniques [35]. With the technique described here access to much smaller nanoparticles will allow the study of the quantum properties of plasmons in a highly dissipative regime. We view this experiment as a shift toward deeply subwavelength quantum optics that will allow otherwise impossible precise characterization of quantum optical properties of confined objects and quantum emitter or plasmon coupling. The experiment presented can be implemented in other widely available TEM and STEM, assuming a suitably designed light collection system [20] is used.

We thank Marcel Tencé for help in setting up the SPADS intensity mapping. We acknowledge Mike Walls, Andréia N. S. Hisi, Luiz F. Zagonel, François Treussart, Christian Colliex, and Odile Stéphan for critical reading of the manuscript and for interesting discussions. This work has received support from the National Agency for Research under the program of future investment TEMPO-CHROMATEM with the Reference No. ANR-10-EQPX-50. The research leading to these results has received funding from the European Union Seventh Framework Programme [No. FP7/2007- 2013] under Grant Agreement No. n312483 (ESTEEM2).

*mathieu.kociak@u-psud.fr

- [1] R. J. Glauber, *Phys. Rev.* **130**, 2529 (1963).
- [2] R. Loudon, *The Quantum Theory of Light* (Oxford University Press, London, 2010).
- [3] W. E. Lamb Jr. and R. C. Retherford, *Phys. Rev.* **72**, 241 (1947).
- [4] D. F. Walls, *Nature (London)* **306**, 141 (1983).
- [5] P. Grangier, G. Roger, and A. Aspect, *Europhys. Lett.* **1**, 173 (1986).
- [6] A. Gruber, A. Drbenstedt, C. Tietz, L. Fleury, J. Wrachtrup, and C. von Borczyskowski, *Science* **276**, 2012 (1997).
- [7] N. Mizouchi, T. Makino, H. Kato, D. Takeuchi, M. Ogura, H. Okushi, M. Nothaft, P. Neumann, A. Gali, F. Jelezko, J. Wrachtrup, and S. Yamasaki, *Nat. Photonics* **6**, 299 (2012).
- [8] B. Lounis and M. Orrit, *Rep. Prog. Phys.* **68**, 1129 (2005).
- [9] R. Kok, W. J. Munro, K. Nemoto, T. C. Ralph, J. P. Dowling, and G. J. Milburn, *Rev. Mod. Phys.* **79**, 135 (2007).
- [10] C. H. Bennet and G. Brassard, *Proceedings of the IEEE International Conference on Computers, Systems and Signal Processing, Bangalore, India, 1984* (IEEE, Bellingham, WA, 1984), Vol. 306, p. 175.
- [11] B. R. Hanbury and R. Q. Twiss, *Nature (London)* **178**, 1046 (1956).
- [12] J. McKeever, A. Boca, A. D. Boozer, R. Miller, J. R. Buck, A. Kuzmich, and H. J. Kimble, *Science* **303**, 1992 (2004).
- [13] S. Kako, S. Santori, K. Hoshino, S. Gtzinger, Y. Yamamoto, and Y. Arakawa, *Nat. Mater.* **5**, 887 (2006).
- [14] P. Spinicelli, S. Buil, X. Quelin, B. Mahler, B. Dubertret, and J.-P. Hermier, *Phys. Rev. Lett.* **102**, 136801 (2009).
- [15] L. Novotny and B. Hecht, *Principles of Nano-Optics* (Cambridge University Press, Cambridge, England, 2006).
- [16] H. Okamoto and K. Imura, *J. Mater. Chem.* **16**, 3920 (2006).
- [17] E. Rittweger, K. Young Han, S. E. Irvine, C. Eggeling, and S. W. Hell, *Nat. Photonics* **3**, 144 (2009).
- [18] J.-J. Greffet, J.-P. Hugonin, M. Besbes, N. D. Lai, F. Treussart, and J.-F. Roch, *arXiv:1107.0502*.
- [19] B. G. Yacobi and D. B. Holt, *Cathodoluminescence Microscopy of Inorganic Solids* (Plenum Press, New York, 1990).
- [20] L. F. Zagonel, S. Mazzucco, M. Tencé, K. March, R. Bernard, B. Laslier, G. Jacopin, M. Tchernycheva, L. Rigutti, F. H. Julien, R. Songmuang, and M. Kociak, *Nano Lett.* **11**, 568 (2011).
- [21] J. Rodriguez-Viejo, K. Jensen, H. Mattoussi, J. Michel, B. Dabbousi, and M. Bawendi, *Appl. Phys. Lett.* **70**, 2132 (1997).
- [22] M. Grundmann, J. Christen, N. N. Ledentsov, J. Böhrer, D. Bimberg, S. S. Ruvimov, P. Werner, U. Richter, U. Gösele, J. Heydenreich, V. M. Ustinov, A. Yu. Egorov, A. E. Zhukov, P. S. Kop'ev, and Zh. I. Alferov, *Phys. Rev. Lett.* **74**, 4043 (1995).
- [23] M. Merano, S. Sonderegger, A. Crottini, S. Collin, P. Renucci, E. Pelucchi, A. Malko, M. H. Baier, E. Kapon, B. Deveaud, and J.-D. Ganière, *Nature (London)* **438**, 479 (2005).
- [24] G. Davies, *Rep. Prog. Phys.* **44**, 788 (1981).
- [25] L. H. G. Tizei and M. Kociak, *Nanotechnology* **23**, 175702 (2012).
- [26] A. Beveratos, S. Kühn, R. Brouri, T. Gacoin, J.-P. Poizat, and P. Grangier, *Eur. Phys. J. D* **18**, 191 (2002).
- [27] P. Y. Yu and M. Cardona, *Fundamentals of Semiconductors* (Springer, New York, 2005).
- [28] F. J. García de Abajo, *Rev. Mod. Phys.* **82**, 209 (2010).
- [29] J. Nelayah, M. Kociak, O. Stephan, F. J. García de Abajo, M. Tencé, L. Henrard, D. Taverna, I. Pastoriza-Santos, L. M. Liz-Marzan, and C. Colliex, *Nat. Phys.* **3**, 348 (2007).
- [30] H. Watanabe, T. Kitamura, S. Nakashima, and S. Shikata, *J. Appl. Phys.* **105**, 093529 (2009).
- [31] X. Bendaña, A. Polman, and F. J. García de Abajo, *Nano Lett.* **11**, 5099 (2011).
- [32] O. Bostanjoglo, R. Elschner, Z. Mao, T. Nink, and M. Weingrtnr, *Ultramicroscopy* **81**, 141 (2000).
- [33] N. D. Browning, M. A. Bond, G. H. Cambell, J. E. Evans, T. LaGrange, K. L. Jungjohann, D. J. Masiel, J. McKeown, S. Mehraeen, B. W. Reed, and M. Santala, *Curr. Opin. Solid State Mater. Sci.* **16**, 23 (2012).
- [34] J. C. Williamson, J. Cao, H. Ihee, H. Frey, and A. H. Zewail, *Nature (London)* **386**, 159 (1997).
- [35] R. Kolesov, B. Grotz, G. Balasubramanian, R. J. Sthr, A. A. L. Nicolet, P. R. Hemmer, F. Jelezko, and J. Wrachtrup, *Nat. Phys.* **5**, 470 (2009).